J Incl Phenom Macrocycl Chem (2013) 75:255–262
DOI 10.1007/s10847-012-0110-3

ORIGINAL ARTICLE

Phase solubility and FTIR-ATR studies of idebenone/sulfobutyl ether β-cyclodextrin inclusion complex

C. Cannavà · V. Crupi · M. Guardo · D. Majolino · R. Stancanelli · S. Tommasini · C. A. Ventura · V. Venuti

Received: 3 October 2011 / Accepted: 8 January 2012 / Published online: 3 March 2012

Abstract The favourable accessibility offered by sulfobutyl ether β-cyclodextrin (SBE-β-CD) for the complexation with idebenone (IDE) has been probed, as a function of temperature, in liquid state, by phase solubility study, and, in solid state, by FTIR-ATR technique. The phase solubility results indicated the formation of a IDE/SBE-β-CD inclusion complex with 1:1 molar ratio (A_L type diagram), whose apparent stability constants at $T = 300$, 310, and 320 K have been estimated according to the Higuchi–Connors method. The formation of the inclusion complex has been confirmed on a freeze-dried and a co-precipitated product by FTIR-ATR spectroscopy, monitoring the changes induced by complexation on some characteristic vibrational bands of IDE. Quantitative studies, performed in a wide T range, from $T = 250$ K to $T = 340$ K, allowed us to extract information on the effect of temperature on the different hydrogen-bonded environments involving host, guest, and crystallization water molecules. Again, complexation is proved to enhance the stability of the guest, at least in the explored T range.

Keywords Idebenone · Sulfobutyl ether β-cyclodextrin · Inclusion complex · Phase-solubility · FTIR-ATR spectroscopy

C. Cannavà (✉) · M. Guardo · R. Stancanelli · S. Tommasini · C. A. Ventura
Dipartimento Farmaco-Chimico, Facoltà di Farmacia, Università di Messina, Viale Annunziata, 98168 Messina, Italy
e-mail: ccannava@alice.it

V. Crupi · D. Majolino · V. Venuti
Dipartimento di Fisica, Facoltà di Scienze MM. FF. NN., Università di Messina, Viale Ferdinando Stagno D'Alcontres 31, Messina, Italy

Introduction

Idebenone [2,3-dimethoxy-5-methyl-6(10-hydroxydecyl)-1,4-benzoquinone, IDE, Fig. 1] is a synthetic short-chain analogue of coenzyme Q10 (CoQ10) [1, 2]. Coenzyme Q (CoQ) is an important membrane antioxidant and essential to the mitochondrial electron transport chain. The idebenone structural similarity with CoQ allows the compound to be used in the therapy of several diseases to increase mitochondrial metabolism. Such is the case in the treatment of patients with Alzheimer, hepatic oxidative stress, brain-vascular diseases and Friedreich's ataxia [3–5]. Due to the capacity of idebenone to prevent lipid peroxidation, the drug protects mitochondrial membrane integrity toward oxidative damage [6]. Its antioxidant properties enable the compound to maintain cellular structures in conditions of brain ischemia and injuries in the central nervous. Idebenone is a highly lipophilic drug with a very low water solubility and the only marketed pharmaceutical formulation is an oral dosage form. The drug solubility and the binding with serum proteins determine a reduced absorption (influenced by food assumption) and a poor bioavailability at the level of the CNS (0.4% of the dose reaches the brain) [7].

In view of this, in therapeutic approaches in which the parenteral route is required (i.e. treatment of pathologies such as brain ischemia or cerebral trauma), the use of IDE is limited for its very low solubility.

Cyclodextrin (CD) is a unique oligosaccharide with hydrophobic cavity and can include and stabilize various organic molecules. Generally, CDs are commonly used in the pharmaceutical industry as complexing agents that increase the water solubility, bioavailability, and stability of poorly soluble drugs [8]. Unfortunately, natural α-CD, β-CD and some methylated CDs produce serious renal damage when administered parenterally [9].

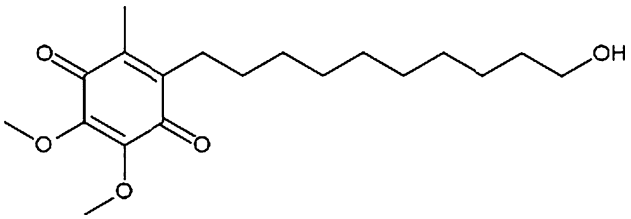

Fig. 1 2,3-Dimethoxy-5-methyl-6(10-hydroxydecyl)-1,4-benzoquinone (Idebenone, IDE)

Sulfobutyl ether β-cyclodextrin (SBE-β-CD) [Fig. 2] is a CD derivative which has shown improved solubility and complexation ability, without the significant toxicity associated with the parent or certain other alkylated CDs [10–13].

Recently, SBE-β-CD is being investigated in drug delivery technology for parenteral [14] and ophthalmic uses [15] and is currently used in four Food and Drug Administration (FDA)-approved injectable products, for IM or IV administration (Geodon®, Abilify®, Vfend®, Nexterone®). In a previous study the inclusion complexes of IDE with natural β-CD and different modified β-CD were studied [16]. The present study is aimed at investigating the possibility of complexation of IDE with SBE-β-CD.

In solution, phase-solubility studies were performed according to the method reported by Higuchi and Connors [17], and the stability constants and the dissolution rates were carried out. In solid phase, Fourier transform infrared spectroscopy in Attenuated Total Reflectance geometry (FTIR-ATR) was used for the physicochemical characterization of the "host–guest" interactions driving the inclusion process. The effect of temperature on the different H-bonded environments contributing to the high frequency vibrational dynamics of the complex will be discussed.

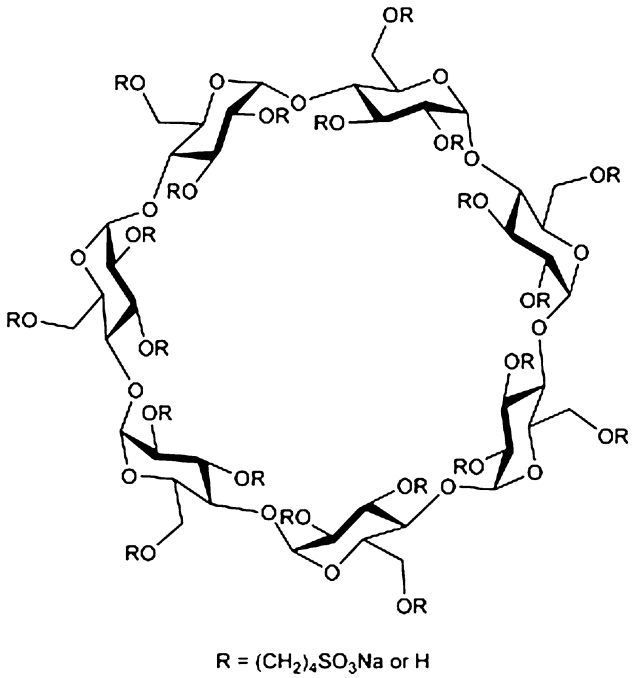

Fig. 2 Sulfobutyl ether β-cyclodextrin [$(SBE)_{7m}$-β-CD]

Experimental

Materials

The following reagents and solvents were used: idebenone [2,3-dimethoxy-5-methyl-6(10-hydroxydecyl)-1,4-benzoquinone, $C_{19}H_{30}O_5$, MW 338.44] was kindly supplied by Wyeth Leaderle S.p.A. (Italia); sulfobutyl ether β-cyclodextrin (SBE-β-CD, average degree of sulfobutyl substitution was seven, average MW 2,612 g/mol) was kindly supplied by CyDex Pharmaceutical (Lenexa, Kansas City, USA). They were employed without any further purification. Water used throughout the study was double-distilled and deionised, then filtered trough 0.22 µm Millipore® GSWP filters (Bedford, USA). Solutions to be analyzed were prior filtered trough 0.45 µm Sartorius Minisart®-SRP 15 PTFE filters (Germany).

Methods

Phase-solubility analysis

Phase-solubility studies were performed using the method described by Higuchi and Connors [17]. A fixed amount of IDE exceeding its solubility, was added to unbuffered aqueous solutions of SBE-β-CD, ($0.0–9.0 \times 10^{-3}$ M) in 10 mL capped tubes, then sonicated in a Bandelin RK 514 water bath (Berlin, Germany) for 15 min. Flasks were sealed to avoid changes due to evaporation and magnetically stirred for 3 days in a Telesystem stirring bath thermostat 15.40 with Telemodul 40 C control unit at $T = 300$, 310, and 320 K, respectively.

After the equilibrium was reached, the suspensions were filtered through Sartorius Minisart®-SRP 15 PTFE 0.20 µm filters. An aliquot from each vial was withdrawn by 1 mL glass syringe (Poulten & Graf GmbH, Germany) and assayed by HPLC (Shidmazu LC-10 AD *VP*) to evaluate the amount of IDE dissolved. Experiments were carried out in triplicate, solubility data were averaged and used to calculate the binding constant for the complexes formation, by HPLC technique.

Continuous variation (Job's plot) method

Equimolar (1×10^{-5} M) methanol/water solutions (55/45 v/v) of IDE and SBE-β-CD were mixed to a fixed volume varying the molar ratio from 0.1 to 0.9, keeping the

molar concentration of the species constant. After stirring for 1 h the absorbance of each solution was measured by UV–Vis spectroscopy (FullTech Instruments, Rome, mod. PG T80) at 280 nm and Δabs was determined as a difference between $abs_{without\ CD}$ and $abs_{with\ CD}$. Then, Δabs • [IDE] was plotted versus R (R = [IDE]/[IDE] + [SBE-β-CD]) [18].

Preparation of the inclusion complex

The inclusion complex of IDE/SBE-β-CD was prepared using co-precipitation method.

An amount of SBE-β-CD (10^{-4} M) was solubilized in water (~50 mL) and IDE was added in the same molar concentration. The mixture was sonicated (30 min) and then magnetically stirred for 3 days and after the suspension was filtered and cooled in the refrigerator (4 °C) for about 3 days. The precipitated complex was filtered, through Sartorius Minisart®-SRP 15 PTFE 0.45 μm filters, and dryied at room temperature.

Dissolution of IDE/SBE-β-CD complex

An accurately weighted amount of the free drug (10 mg) or a corresponding amount in the complex were suspended in water (~50 mL), maintained at 37.0 ± 0.5 °C and magnetically stirred at 100 rpm. Samples (1 mL) were removed at regular intervals and after filtration analysed using HPLC as described below. The medium was reconstituted with fresh water and the data were corrected for the operated dilutions. The experiments were carried out in triplicate.

HPLC assay

The concentrations of IDE in the phase solubility and dissolution studies were carried out by reverse phase HPLC method (Shimadzu HPLC Prominence LC-20AB pump). Twenty microliters of samples were injected into Discovery® C18 column (250 × 4.6 mm i.d., 5 μm, Supelco). Flow rate 0.7 mL/min was employed for the mobile phase consisting of water:acetonitrile (25:75 v/v). IDE was detected at 282 nm using an UV detector (Shimadzu UV–Vis detector SPD-20A).

FTIR-ATR spectroscopy

FTIR-ATR spectra were recorded in the 400 ÷ 4,000 cm^{-1} region, in the temperature range extending from 250 to 340 K. Measurements were performed by a Bomem DA8 Fourier transform spectrometer, operating with a Globar source, in combination with a KBr beamsplitter, a DTGS/KBr detector. It was equipped with a Golden Gate diamond ATR system, just based on the ATR technique [19]. Spectra were recorded in dry atmosphere, by co-addition of 100 repetitive interferograms at a resolution of 4 cm^{-1} and then normalized for taking into account the effective number of absorbers. To check a possible unwanted effect induced by wetting and/or drying phenomena when the sample holder was filled with dry nitrogen, IR spectra in the presence and absence of air were compared without showing any significant difference. Any smoothing was applied, and spectroscopic manipulation such as baseline adjustment and normalization were performed using the Spectracalc software package GRAMS (Galactic Industries, Salem, NH, USA). For the analysis of the 3,000 ÷ 3,800 cm^{-1} region, typical of the O–H stretching intramolecular vibrational mode, that required a band decomposition procedure, second derivative computations have been used for evaluating the wavenumbers of the maxima of the different sub-bands. Multiple curve fitting into Voigt profiles were then applied to the experimental profiles based on these wavenumber values, by using the routine provided in the PeakFit 4.0 software package. The statistical parameters defined in the software manual were used as a guide to "best-fit", and allowed to vary upon iteration until converging solution is reached. The "best-fit" is characterized by $r^2 \sim 0.9999$ for all the investigated systems.

Results and discussion

In solution studies

The phase solubility diagrams for IDE with SBE-β-CD at T = 300 K, T = 310 K, and T = 320 K, within the tested concentration range of cyclodextrin, are shown in Fig. 3a–c. They display a linear increase of solubility of IDE with the increasing concentration of SBE-β-CD, indicating favourable interaction between host and guest giving rise to the formation of a soluble complex. In particular, A_L type diagrams were obtained, and since the slope of the diagrams is less than 1, the stoichiometry of the complex was assumed to be 1:1 over the concentration range studied. Then, the stability constants, K_c, were calculated from the straight-line portion of the phase-solubility diagram [17], according to the following equation: $K_c = \alpha/S_0(1-\alpha)$, where α is the slope of the linear plot reporting the amount of complexed IDE as a function of CD and S_0 is the solubility of IDE in water. A smaller K_c value indicates too weak an interaction, whereas a larger value indicates the possibility of limited release of drug from the complex thereby interfering with drug absorption. In particular, the highest value for the stability constant was obtained for the complex at 300 K (K_c = 13,666 M^{-1}) and then, in order, at 310 K (K_c = 11,397 M^{-1}) and 320 K (K_c = 6,141 M^{-1}). It is clear that the stability constants decreased when the heat was provided

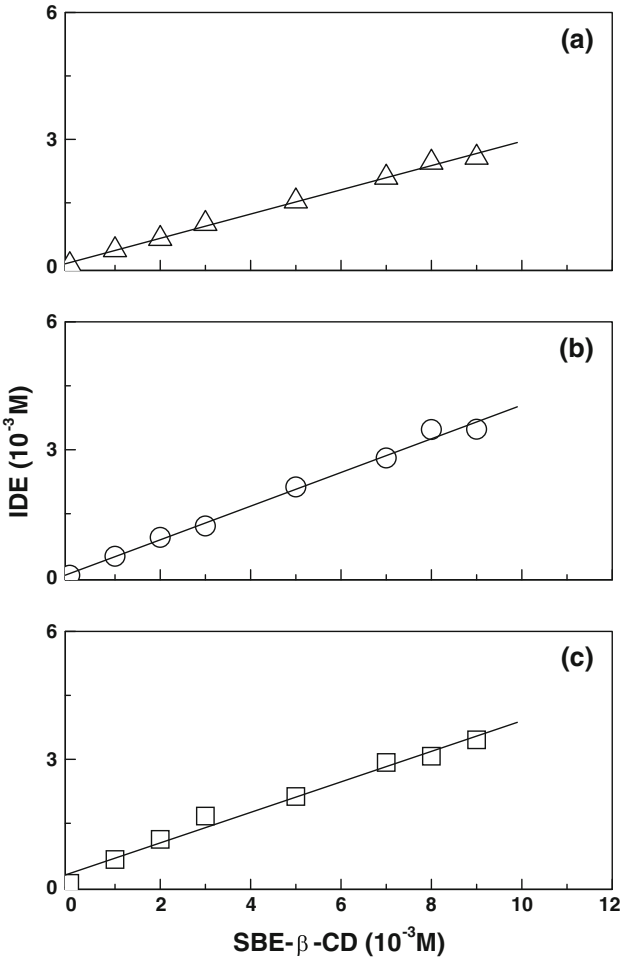

Fig. 3 Phase-solubility diagram of IDE in the presence of increasing concentration of SBE-β-CD in water at $T = 300$ K (**a**), $T = 310$ K (**b**), and $T = 320$ K (**c**)

to the systems, indicating that there was exothermic process in all systems.

Stoichiometry of the complex was confirmed by Job's plot, considering variation of UV–Vis spectra of IDE in the presence of SBE-β-CD. The UV–Vis spectrum of IDE shows two absorption bands, at 280 and 408 nm [16]. In Fig. 4 was reported the influence of increasing amounts of SBE-β-CD on the 280 nm band, showing a small bathochromic shift (1 nm) and a significant hypochromic shift. As reported by other authors [20–22] the influence of CD on UV bands of a drug is due to the complexation with CD cavity. The Job's plot obtained from absorbance measures was shown in Fig. 5. A maximum value at $R = 0.5$ and a highly symmetrical shape evidenced the presence of a complex with 1:1 stoichiometry within the range of the investigated concentrations. These results are in agreement with the phase solubility studies.

The increased solubility of IDE due to the SBE-β-CD complexation, significantly influences its dissolution rate.

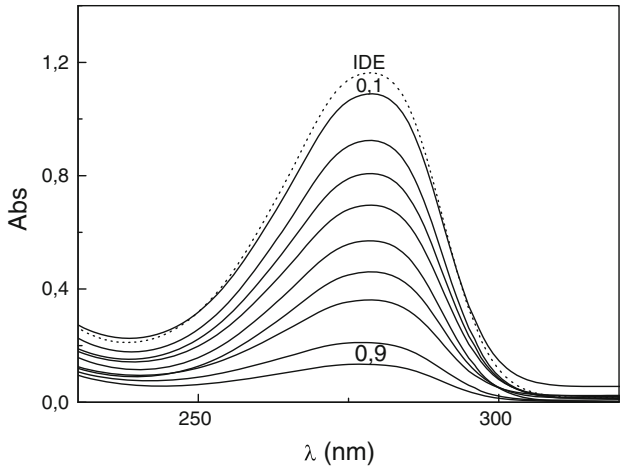

Fig. 4 UV–Vis spectra of 280 nm band of IDE (*dot line*) free and in presence of increasing amount of SBE-β-CD (*solid lines*)

The Fig. 6 showed faster dissolution of IDE/SBE-β-CD complex with respect to free drug.

FTIR-ATR absorption studies

Complexation between SBE-β-CD and IDE is accompanied by changes in the IR spectra of the inclusion complex as compared with the physical mixture (a simple blending in 1:1 molar ratio without complexation) and individual components [23]. Figure 7 shows the FTIR-ATR spectra of IDE, SBE-β-CD, their 1:1 physical mixture, and their 1:1 inclusion complex, in the solid state, recorded within 3,800 ÷ 600 cm^{-1} wavenumber range, at $T = 300$ K as an example.

The IR spectrum of IDE reveals, as main features, the presence of a peak at ~3,570 cm^{-1}, assigned to O–H stretching vibration, a double-peak at ~2,918 and ~2,842 cm^{-1}, assigned to C–H stretching vibration, and a double-peak at ~1,647 and ~1,603 cm^{-1}, corresponding, respectively, to the carbonyl C=O and ring C=C stretching vibrations. Going on, a multiple-peak region is revealed, extending from ~1,500 to ~1,000 cm^{-1}, ascribed to the C–C stretching vibration (~1,461 and ~1,429 cm^{-1}), probably convoluted with CH_2 bending vibrations of the alkyl chain, in plane OH bending vibration (~1,375 cm^{-1}), CH rocking stretching vibration of the ring convoluted with C–O stretching vibrations (from ~1,270 to ~1,000 cm^{-1}). Finally, the intense bands that appears in the 900 ÷ 500 cm^{-1} region correspond to the out-of-plane bending of aromatic C–H bonds.

The spectrum of SBE-β-CD is mainly characterized by intense bands at 3,700 ÷ 3,000 cm^{-1} due to O–H stretching vibration, overlapped with the band associated to the vibration of the –CH and –CH_2– groups that appears in the 3,000 ÷ 2,800 cm^{-1} region. The band at ~1,644 cm^{-1}

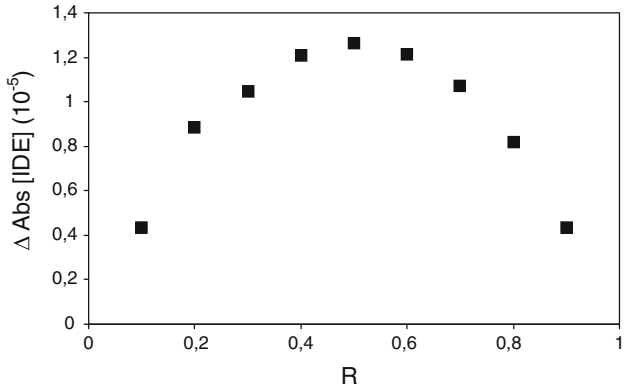

Fig. 5 Continuous variation plot (Job's plot) for the complexation of IDE with SBE-β-CD from absorbance measurements

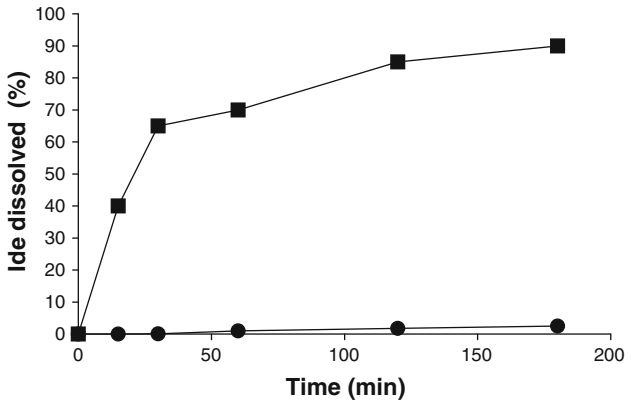

Fig. 6 Dissolution profiles of free (*closed circles*) and complexed (*closed squares*) IDE

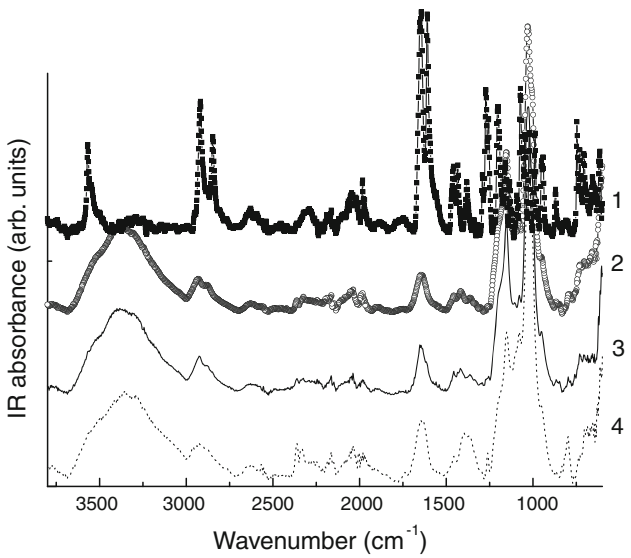

Fig. 7 Solid phase FTIR-ATR spectra of IDE (*closed squares*, 1), SBE-β-CD (*open circles*, 2), 1:1 IDE + SBE-β-CD physical mixture (*solid line*, 3), 1:1 IDE/SBE-β-CD inclusion complex (*dotted line*, 4), at $T = 300$ K

will reflect the δ-HOH bending of water molecules attached to CD, whereas the peaks at 1,148 and 1,016 cm^{-1} are respectively ascribed to C–H and C–O stretching vibrations.

The physical mixture showed approximately the superposition of drug and cyclodextrin spectra, whereas the inclusion complex displayed frequency shifts, broadening and or disappearing of the IR bands characteristic of the pure drug, indicating alteration in bond strength and length in the drug because of the activation of some "host–guest" interaction [24, 25].

Our attention has been mainly focused on the O–H stretching vibration, well evident in the 3,700 ÷ 3,000 cm^{-1} spectral range, where contributions coming from primary and secondary OH groups of SBE-β-CD, of IDE, of interstitial and intracavity crystallization water molecules are present, overlapped [26]. In the 3,000 ÷ 2,800 cm^{-1} range are also evident the C–H stretching bands. Second derivative computation and curve fitting procedure have been used in order to separate the unresolved bands present in this spectral range.

First of all, because of the partial overlapping of O–H and C–H stretching bands, it was necessary to fit the whole spectrum in order to separate the O–H stretching region. Voigts bands were used as fitting functions, and the contributions due to symmetric and antisymmetric methyl stretches needed to be subtracted from the total fits. More detailed fits were subsequently performed just in the O–H stretching region. According to a well-established procedure already used for a variety of systems [27–29], by the second derivative computation, whose results are not reported here, we evaluated the wavenumber of the maxima for the band components, by looking at the minima in the second derivative profile. The curve fitting procedure was applied to the experimental profiles based on these wavenumber values. In particular, five Voigt peaks have been used, and the obtained sub-bands are shown, respectively, in Figs. 8 and 9 for SBE-β-CD + IDE physical mixture and IDE/SBE-β-CD inclusion complex at $T = 250$ K and $T = 320$ K, as examples.

The main fit parameters, i.e. centre-frequency, percentage intensity, and vibrational assignment (performed on the basis of previous studies [26–30]) of the various sub-bands, are reported in Table 1 for all the analysed temperatures.

By increasing T, a destructuring effect on the hydrogen bond network is revealed on both physical mixture and inclusion complex. It is testified by the decreasing of the population (as expressed by the percentage intensity) of water molecules retained in the interstices among different SBE-β-CD molecules and linked, via H-bond, to the macrocycle and/or to IDE. At the same time, in fact, a diminishing of the number of IDE molecules linked in a H-bond

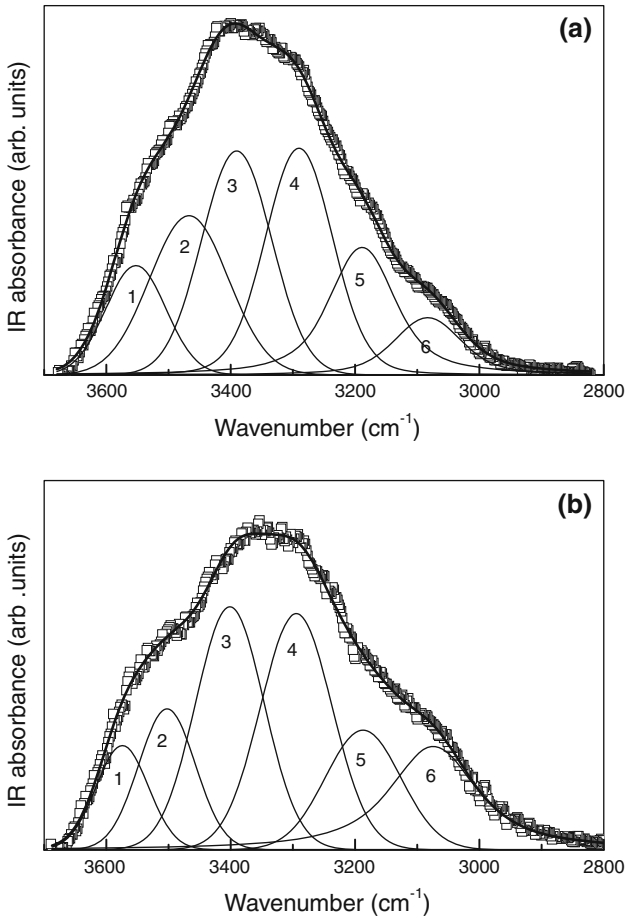

Fig. 8 Fitting results for the O–H stretching region for 1:1 IDE + SBE-β-CD physical mixture (**a**) and 1:1 IDE/SBE-β-CD inclusion complex (**b**) at $T = 250$ K, as example

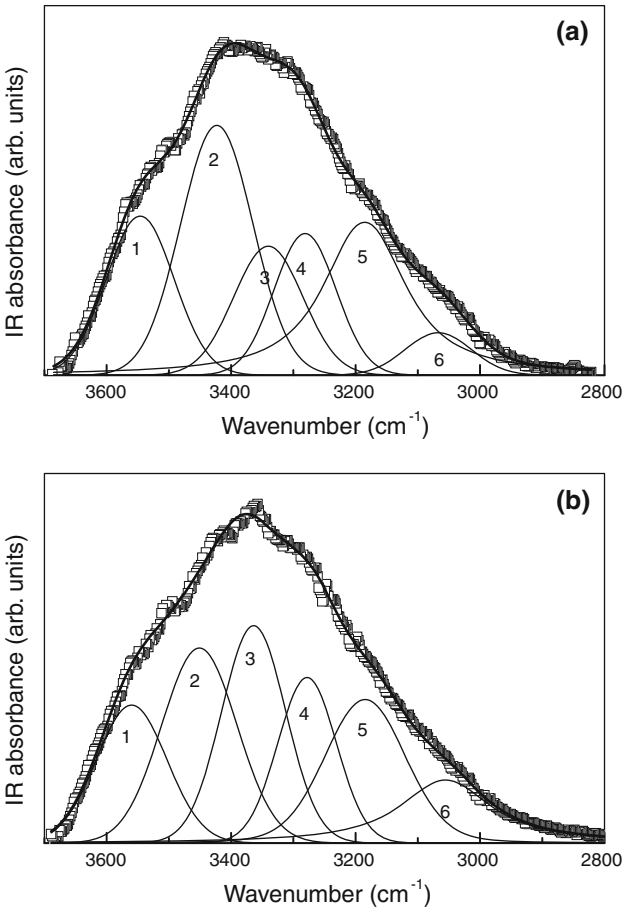

Fig. 9 Fitting results for the O–H stretching region for 1:1 IDE + SBE-β-CD physical mixture (**a**) and 1:1 IDE/SBE-β-CD inclusion complex (**b**) at $T = 320$ K, as example

scheme is revealed. On the contrary, the contribution coming from primary and secondary OH groups of SBE-β-CD become always more relevant with T, as expected.

By complexation we observe, first of all, that the highest frequency sub-bands, i.e. ω_1, ω_2, and ω_3, move further towards higher wavenumbers passing from physical mixture to inclusion complex, indicating a reduced co-operativity of the H-bonded environments these O–H groups belong to.

The inclusion process affect water molecules inside the cyclodextrin cavity, that are forced out of the torus by the guest entrance, and reorganize a different, interstitial, H-bond environment.

The comparison between IDE + SBE-β-CD physical mixture and IDE/SBE-β-CD inclusion complex spectra (see Fig. 7 at $T = 300$ K as example) show also significant changes in the C–H stretching region, indicative of the existence of some host–guest interaction involving these functional groups. Going to lower wavenumbers, as main results, an enlargement of the peak associated to the C=O stretching vibration of IDE ($\sim$1,647 cm^{-1}) is first of all observed passing from physical mixture to inclusion complex, indicating a hindering of this vibration due to the cyclodextrin cavity. At the same time, the peak associated to the C=C stretching vibration of IDE ($\sim$1,603 cm^{-1}), still evident as a low-frequency shoulder in the physical mixture spectrum, almost disappears for the inclusion complex, probably owing to a restriction of these groups due to the cyclodextrin cavity.

The peak at $\sim$1,429 cm^{-1} in IDE spectrum, ascribed to C–C stretching vibration, is still present at the same frequency, in the physical mixture, whereas exhibits a low-frequency shift for the inclusion complex, together with a change in the relative intensity with respect to the other C–C stretching peak ($\sim$1,461 cm^{-1}) and the in plane OH bending vibration ($\sim$1,375 cm^{-1}), and an overall broadening of the band. The low-frequency shift reveals a weakening of the corresponding bond, may be due to a more intense host–guest association "seen" by the C–C group as a consequence of the more or less deep inclusion of the guest inside the host cavity.

In the C–O stretching region, the high-frequency shoulder at $\sim$1,198 cm^{-1}, well evident in the physical

Table 1 Vibrational assignment and main fitting parameters, i.e. wavenumber (ω, cm^{-1}) and percentage intensity (I, %), of the FTIR-ATR sub-bands in the O–H stretching region of IDE + SBE-β-CD physical mixture and IDE/SBE-β-CD inclusion complex in the whole explored T range

T (K)	O–H stretching intra-cavity H_2O		O–H stretching primary OH groups		O–H stretching interstitial H_2O		O–H stretching O–H groups of IDE		O–H stretching secondary OH groups		O–H stretching interstitial H_2O	
	ω_1 (cm^{-1})	I_1 (%)	ω_2 (cm^{-1})	I_2 (%)	ω_3 (cm^{-1})	I_3 (%)	ω_4 (cm^{-1})	I_4 (%)	ω_{5c} (cm^{-1})	I_5 (%)	ω_6 (cm^{-1})	I_6 (%)
IDE + SBE-β-CD physical mixture												
250	3552.5	10	3467.1	19.0	3390.3	23.7	3290.2	24.2	3188.7	16.1	3083.1	6.9
260	3550.4	12.5	3449.0	22.0	3383.5	21.8	3286.6	20.4	3184.3	16.7	3074.3	6.4
270	3551.2	12.6	3444.2	22.5	3387.5	21.7	3287.8	20.0	3184.0	17.4	3072.4	5.8
280	3549.0	13.9	3440.6	22.7	3363.7	19.3	3280.7	18.7	3182.1	20.1	3066.1	5.1
290	3544.2	15.0	3433.3	22.9	3351.3	18.6	3272.0	17.9	3173.1	21.0	3063.8	4.5
300	3542.9	16.4	3429.5	23.0	3346.1	16.8	3267.6	17.0	3169.0	22.4	3057.8	4.4
310	3548.1	16.5	3418.5	24.3	3341.0	13.8	3269.1	14.3	3177.4	25.5	3062.8	5.5
320	3546.2	16.1	3423.0	26.9	3340.2	13.3	3281.1	13.1	3185.5	26.3	3067.1	4.2
IDE/SBE-β-CD inclusion complex												
250	3574.3	8.0	3502.3	11.6	3401.4	24.3	3294.5	24.7	3187.1	13.2	3074.1	18.2
260	3564.7	10.1	3477.5	13.6	3378.7	23.7	3276.0	21.9	3177.1	13.4	3072.8	17.3
270	3563.6	10.6	3473.7	15.5	3375.3	22.9	3272.2	20.5	3166.2	13.9	3067.9	16.6
280	3566.7	10.8	3477.2	16.2	3378.6	22.5	3278.7	20.7	3175.0	14.0	3069.1	15.8
290	3564.0	11.4	3467.3	17.2	3370.9	22.0	3273.6	19.3	3165.2	14.8	3061.0	15.3
300	3567.6	11.1	3465.7	17.7	3365.5	21.3	3268.0	18.0	3159.6	17.2	3058.1	14.7
310	3563.5	13.0	3456.4	19.7	3369.9	21.1	3282.9	14.8	3190.6	17.6	3066.9	13.8
320	3559.9	14.2	3451.0	21.4	3363.7	20.3	3277.9	14.1	3184.6	17.8	3055.4	12.2

mixture spectrum, reduces in intensity and enlarges in the complex. Again, this vibration appears hindered, because of the close fitting of IDE into the SBE-β-CD cavity.

Finally, temperature seems not to have any relevant effect on the investigated complex in solid state, at least in the explored range. In Fig. 10 we report the FTIR-ATR spectra of the IDE/SBE-β-CD inclusion complex at $T = 250$ K, $T = 290$ K, and $T = 320$ K, as examples. The spectral profiles appear almost completely overlapped, revealing a thermal stability of the solid system, probably induced by the activation of the "host–guest" interactions involving the aforementioned functional groups.

These results shed light into complexation mechanism of IDE and SBE-β-CD in solid phase, evidencing the inclusion complex as a new phase in a more amorphous state. Corroborated by other experimental techniques and theoretical approaches, they are crucial for the determination of the complex geometry.

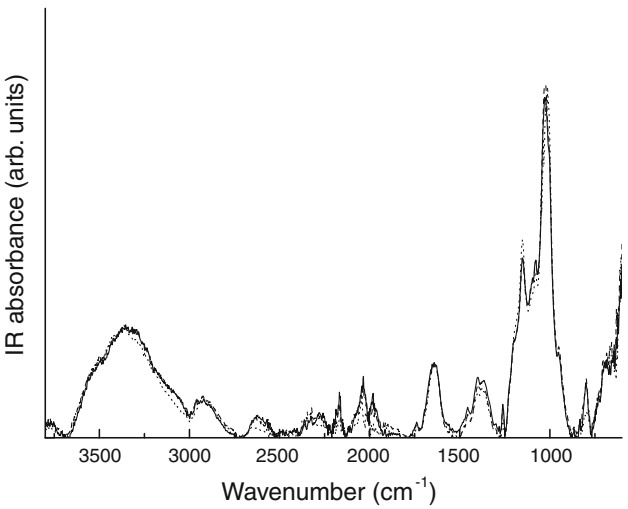

Fig. 10 Solid phase FTIR-ATR spectra of 1:1 IDE/SBE-β-CD inclusion complex at $T = 250$ K (*solid line*), $T = 290$ K (*dashed line*) and $T = 320$ K (*dotted line*)

Conclusions

Phase solubility analysis and FTIR-ATR spectroscopy have been used to study the inclusion complex formed by IDE and SBE-β-CD both in liquid and solid phase.

In liquid state, the results from the phase-solubility diagram and Job's plot evidence that the aqueous solubility of the drug was enhanced considerably by the formation of a 1:1 complex. The equilibrium constants were evaluated by the phase-solubility method as a function of temperature.

In solid state, remarkable changes in some of the vibrational bands characteristic of the guest were detected in the spectrum of the inclusion complex if compared to physical mixture, indicative of the involving of the corresponding

functional groups in "host–guest" interactions driving the formation of a binary inclusion complex as a new solid phase, amorphous in character. From the results, the escape of water molecules from inside the cavity, when the guest penetrates, and the consequent structural rearrangement of the H-bonded scheme involving host and guest, whose evolution in temperature has been quantitatively investigated, can reasonably explain the complexation mechanism. The observed "host–guest" interactions are hypothesized to be responsible of the thermal stability of the complex, observed in a wide temperature range.

The observed enhancement on the physicochemical properties of the guest, i.e. solubility, dissolution rate and probably bioavailability, can have a strong impact when evaluating the biopharmaceutical effects of IDE/SBE-β-CD system as a new drug delivery product.

References

1. Degli Esposti, M., Ngo, A., Ghelli, A., Benelli, B., Carelli, V., McLennan, H., Linnane, A.W.: The interaction of Q analogs, particularly hydroxydecyl benzoquinone (idebenone), with the respiratory complexes of heart mitochondria. Arch. Biochem. Biophys. **330**, 395–400 (1996)
2. Geromel, V., Darin, N., Chrétien, D., Bénit, P., DeLonlay, P., Rötig, A., Munnich, A., Rustin, P.: Coenzyme Q(10) and idebenone in the therapy of respiratory chain diseases: rationale and comparative benefits. Genet. Metab. **77**, 21–30 (2002)
3. Gutzmann, H., Hadler, D.: Sustained efficacy and safety of idebenone in the treatment of Alzheimer's disease: update on a 2-year double-blind multicentre study. J. Neural Transm. Suppl. **54**, 301–310 (1998)
4. Thal, L.J., Grundman, M., Berg, J., Ernstrom, K., Margolin, R., Pfeiffer, E., Weiner, M.F., Zamrini, E., Thomas, R.G.: Idebenone treatment fails to slow cognitive decline in Alzheimer's disease. Neurology **61**, 1498–1502 (2003)
5. Schols, L., Meyer, C.h., Schmid, G., Wilhelms, I., Przuntek, H.: Therapeutic strategies in Friedreich's ataxia. J. Neural Transm. Suppl. **68**, 135–145 (2004)
6. Genova, M.L., Pich, M.M., Biondi, A., Bernacchia, A., Falasca, A., Bovina, C., Formiggini, G., Parenti Castelli, G., Lesnaz, G.: Mitochondrial production of oxygen radical species and the role of coenzyme Q as an antioxidant. Exp. Biol. Med. **228**, 506–513 (2003)
7. Gillis, J.C., Benefield, P., McTavish, D.: Idebenone. A review of its pharmacodynamic and pharmacokinetic properties, and therapeutic use in age-related cognitive disorders. Drugs Aging **5**, 133–152 (1994)
8. Loftsson, T., Jarho, P., Masson, M., Jarvinen, T.: Cyclodextrins in drug delivery. Expert. Opin. Drug Deliv. **2**, 335–351 (2005)
9. Frank, D.W., Gray, J.E., Weaver, R.N.: Cyclodextrin nephrosis in the rat. Am. J. Pathol. **83**, 367–382 (1976)
10. Irie, T., Uekama, K.: Pharmaceutical application of cyclodextrins. III. Toxicological issues and safety evaluation. J. Pharm. Sci. **86**, 147–162 (1997)
11. Rajewski, R.A., Traiger, G., Bresnahan, J., Jaberaboansari, P., Stella, V.J., Thompson, D.O.: Preliminary safety evaluation of parenterally administered sulfoalkyl ether β-cyclodextrin derivatives. J. Pharm. Sci. **84**, 927–932 (1995)
12. Stella, V.J., Rajewski, R.A.: Cyclodextrins: their future in drug formulation and delivery. Pharm. Res. **14**, 556–567 (1997)
13. Luna, E., Vander Velde, D.G., Tait, R.J., Thompson, D.O., Rajewski, R.A., Stella, V.J.: Isolation and characterization by NMR spectroscopy of three monosubstituted 4-sulfobutyl ether derivatives of cyclomaltoheptaose (β-cyclodextrin). Carbohydr. Res. **299**, 111–118 (1997)
14. Holvoet, C., Heyden, Y.V., Plaizier-Vercammen, J.: Inclusion complexation of diazepam with different cyclodextrins in formulations for parenteral use. Pharmazie **60**, 598–603 (2005)
15. Järvinen, T., Järvinen, K., Urtti, A., Thompson, D., Stella, V.J.: Sulfobuthyl ether beta-cyclodextrin (SBE-beta-CD) in eyedrops improves the tolerability of a topically applied pilocarpine prodrug in rabbits. J. Ocul. Pharmacol. Ther. **11**, 95–106 (1995)
16. Puglisi, G., Ventura, C.A., Fresta, M., Vandelli, M.A., Cavallaro, G., Zappalà, M.: Preparation and physico-chemical study of inclusion complexes between idebenone and modified β-cyclodextrin. J. Incl. Phenom. **24**, 193–210 (1996)
17. Higuchi, T., Connors, K.A.: Phase solubility techniques. Adv. Anal. Chem. Instr. **4**, 117–212 (1965)
18. Gibaud, S., Zirar, S.B., Mutzenhardt, P., Fries, I., Astier, A.: Melarsoprol-cyclodextrins inclusion complexes. Int. J. Pharm. **306**, 107–121 (2005)
19. Maréchal, Y.: Observing the water molecule in macromolecules and aqueous media using infrared spectrometry. J. Mol. Struct. **648**, 27–47 (2003)
20. Szejtli, J.: Cyclodextrins and their inclusion compounds. Akademiai Kiado, Budapest (1982)
21. Dotsikas, Y., Kontopanou, E., Allagiannis, C., Loukas, Y.L.: Interaction of 6-p-toluidinylnaphthalene-2-sulphonate with β-cyclodextrin. J. Pharm. Biomed. Anal. **23**, 997–1003 (2000)
22. Jara, F., Dominquez, M., Rezende, M.C.: The interaction of solvatochromic pyridiniophenolates with cyclodextrins. Tetrahedron **62**, 7817–7823 (2006)
23. Aramă, C., Nicolescu, C., Nedelcu, A., Monciu, C.M.: Synthesis and characterization of the inclusion complex between repaglinide and sulfobutylether-β-cyclodextrin (Captisol®). J. Incl. Phenom. Macrocycl. Chem. **70**, 421–428 (2011)
24. Crupi, V., Guella, G., Majolino, D., Mancini, I., Rossi, B., Stancanelli, R., Venuti, V., Verrocchio, P., Viliani, G.: T-dependence of the vibrational dynamics of IBP/diME-β-CD in solid state: a FT-IR spectral and quantum chemical study. J. Mol. Struct. **972**, 75–80 (2010)
25. Crupi, V., Majolino, D., Venuti, V., Guella, G., Mancini, I., Rossi, B., Verrocchio, P., Viliani, G., Stancanelli, R.: Temperature effect on the vibrational dynamics of cyclodextrin inclusion complexes: investigation by FTIR-ATR spectroscopy and numerical simulation. J. Phys. Chem. A **114**, 6811–6817 (2010)
26. Gavira, J.M., Hernanz, A., Bratu, I.: Dehydration of β-cyclodextrin: an IR ν(OH) band profile analysis. Vib. Spectrosc. **32**, 137–146 (2003)
27. Crupi, V., Ficarra, R., Guardo, M., Majolino, D., Stancanelli, R., Venuti, V.: UV–vis and FTIR-ATR spectroscopic techniques to study the inclusion complexes of genistein with β-cyclodextrins. J. Pharm. Biomed. Anal. **44**, 110–117 (2007)
28. Stancanelli, R., Ficarra, R., Cannavà, C., Guardo, M., Calabrò, M.L., Ficarra, P., Ottanà, R., Maccari, R., Crupi, V., Majolino, D., Venuti, V.: UV–vis and FTIR-ATR characterization of 9-fluorenon-2-carboxyester/(2-hydroxypropyl)-β-cyclodextrin inclusion complex. J. Pharm. Biomed. Anal. **47**, 704–709 (2008)
29. Cannavà, C., Crupi, V., Ficarra, P., Guardo, M., Majolino, D., Stancanelli, R., Venuti, V.: Physicochemical characterization of coumestrol/β-cyclodextrins inclusion complexes by UV–vis and FTIR-ATR spectroscopies. Vib. Spectrosc. **48**, 172–178 (2008)
30. Bratu, I., Veiga, F., Fernandes, C., Hernanz, A., Gavira, J.M.: Infrared spectroscopic study of triacetyl-β-cyclodextrin and its inclusion complex with nicapiridine. Spectroscopy **18**, 459–467 (2004)